

3.5.1. PLANETS EXPLORATION

3.5.1.1. Discovery of an aurora on Mars. SPICAM Mars Express

Here we report the discovery of an aurora in the martian atmosphere, using the ultraviolet spectrometer SPICAM on board Mars Express. In the high-latitude regions of Earth, aurorae are manifestation of the interaction between electrically charged particles with the neutral upper atmosphere, as they precipitate along magnetic field lines. Auroral activity has been found on all four giant planets possessing a magnetic field (Jupiter, Saturn, Uranus and Neptune), as well as on Venus, which has no magnetic field. But martian aurora corresponds to a distinct type of aurora not seen before in the Solar System: it is unlike aurorae at Earth and the giant planets, which lie at the foot of the intrinsic magnetic field lines near the magnetic poles, and unlike venusian auroras, which are diffuse, sometimes spreading over the entire disk. Instead, the martian aurora is a highly concentrated and localized emission controlled by magnetic field anomalies in the martian crust. The main emissions in the auroral spectrum are associated with the CO and CO⁺₂, long observed between 118 and 310 nm. The altitude of the observed emission is 115-145 km and the horizontal size is about 30 km. The duration of the spikes was usually more than 8 s. It is notable that the region the largest martian magnetic crustal anomalies is determined above for the auroral emission.

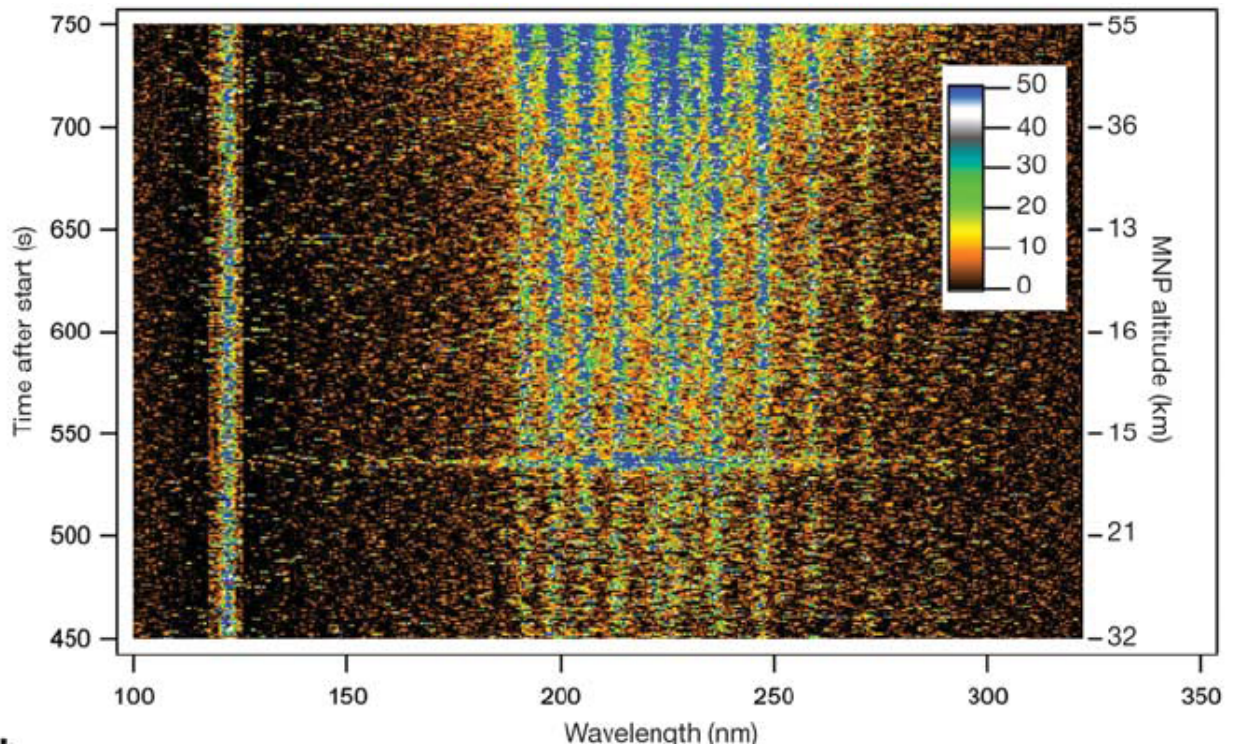


Fig. 1. Time variation of the martian nightglow intensity. It contains the H Lyman- α emission at 121.6 nm and a well structured band (190–270 nm), identified as NO. There is however also a strong peak around time 535 s, it differs from the typical NO spectrum and contains bands CO and CO⁺₂

3.5.1.2. The observation of nightglow in the upper atmosphere of Mars: the NO bands in UV and implications for atmospheric transport. SPICAM Mars Express

We detected light emissions in the nightside martian atmosphere with the SPICAM (spectroscopy for the investigation of the characteristics of the atmosphere of Mars) ultraviolet (UV) spectrometer on board the Mars Express. The UV spectrum of this nightglow is composed of the (expected) H Lyman α emission (121.6 nm), and of the δ and γ bands of nitric oxide (NO, 190-270 nm) produced when N and O atoms combine to produce NO (nitric oxide) molecule. N and O atoms are produced by EUV photo-dissociation of O₂, CO₂ and N₂ in the dayside upper atmosphere, and transported on the night side. The NO emission is brightest in the winter south polar night, which can be explained by downward transport of air in this region permanently in the night, and where CO₂ condenses at ground level. It opens a new way to study the general circulation mechanisms by remote sensing of the upper atmosphere from Mars orbiters. This Mars emission is similar to the Venus UV NO nightglow which was discovered on Venus.

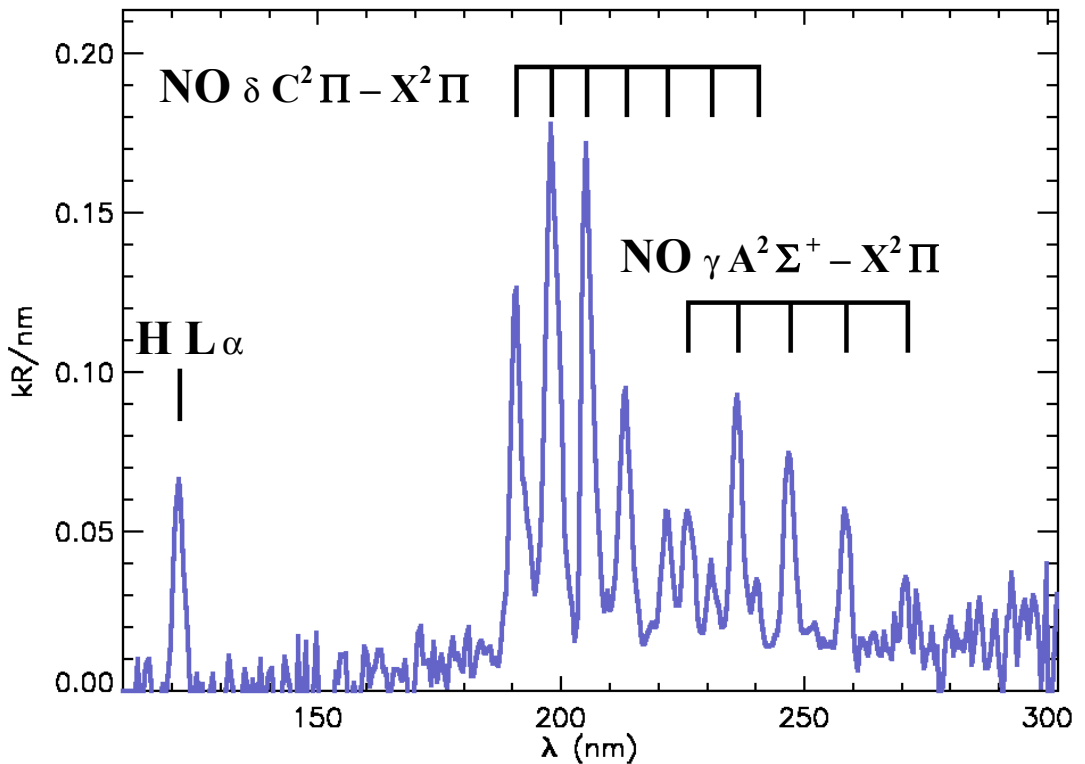


Fig. 2. Spectrum of light emissions in the nightside martian atmosphere is detected with the SPICAM on board the Mars Express. Except for $L\alpha$ at 121.6 nm, all the observed lines coincide precisely with the main NO and vibrational state transitions

The SPICAM on board the Mars Express consists of separate ultraviolet (UV) and near-infrared spectrometers dedicated primarily to the study of the atmosphere of Mars. The device is constructed by efforts of three organizations in France, in Belgium and in Institute of space researches (IKI) in Moscow.

3.5.1.3. Gravity waves and the CO₂ clouds in the polar region at late winter. OMEGA and PFS Mars Express

The OMEGA image of the polar region in the O₂ 1.27 μm emission band at late winter reveals wave-like structures in the latitude range from around 70°N up to terminator (80°N). The crests of gravity waves are parallel to terminator, and their wavelength changes from several tens of km up to 100 – 150 km near terminator. Gravity wave patterns are found also in the maps of the 1.43 μm CO₂ ice and the 1.52 μm H₂O ice absorption bands (Figs. b, c). They show anticorrelation between H₂O and CO₂ ices, indicating to predominance of clouds, consisting from one or another ice. Temperature profiles, obtained from the simultaneous PFS observations, show that the CO₂ condensation occurs at latitudes exceeding 70°N below 20 km altitude in the atmosphere. The CO₂ clouds may be observed even on the day side not far from terminator.

The boundary of the CO₂ polar cap (where the CO₂ ice is observed on the surface) is found at around 62°N. Thus, anticorrelation between intensities of the CO₂ and H₂O ices at < 70°N indicates that the CO₂ ice is observed on the surface (the temperature profiles, retrieved from the PFS data show that temperature of the atmosphere is too high for CO₂ condensation in the atmosphere at these latitudes). The surface may be seeing, when the H₂O clouds of polar vortex absent or have reduced opacity: bright H₂O features are connected to the polar vortex. Bright CO₂ features indicate that we see the surface, covered by CO₂ ice.

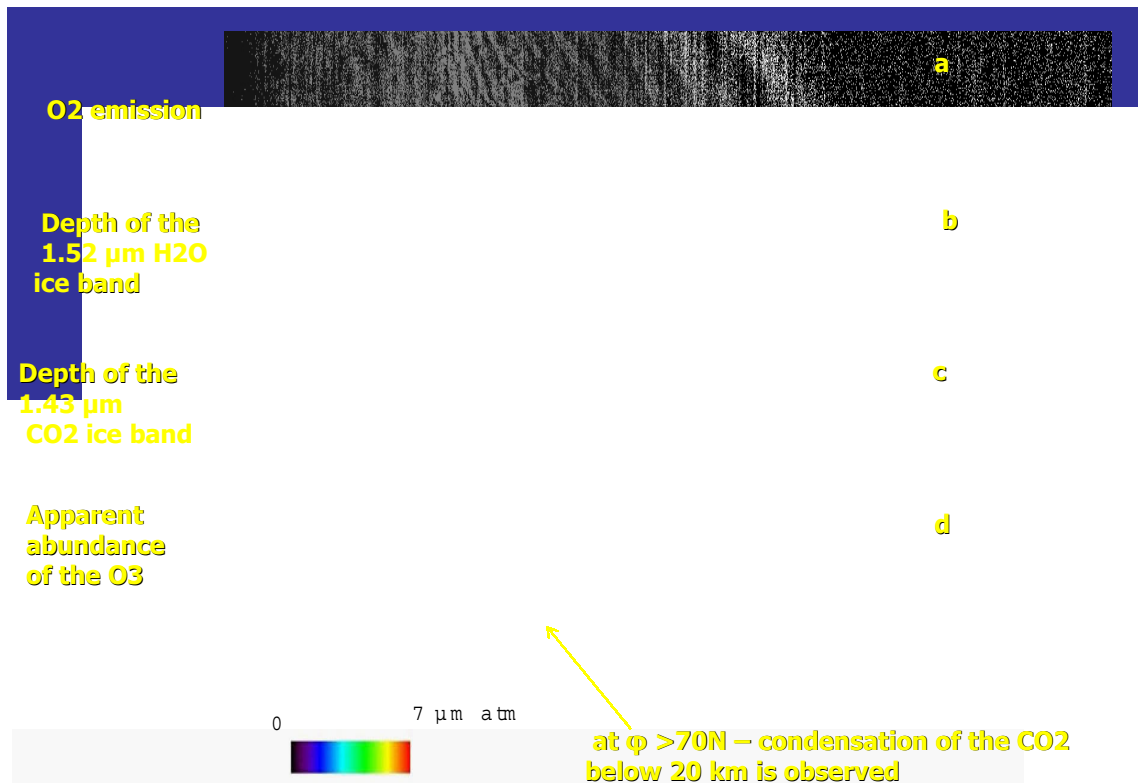


Fig. 3. OMEGA images: a — Equivalent width of the O₂ 1.27 μm emission band; b — relative depths of the 1.52 μm H₂O ice band and c — the 1.43 μm CO₂ ice absorption band; d — apparent ozone abundance

The gravity waves activity correlates with presence of the CO₂ clouds in the atmosphere. These waves are not connected to the relief.

3.5.1.4. Ozone vertical profiles from OMEGA limb measurements

Although the OMEGA resolution is not enough to resolve the O₂ day glow band at 1.27 μm , the spectral data allow estimation the total intensity of this emission and the high spatial resolution of OMEGA (up to 1 km at the limb) enables to obtain the vertical profile of the emission. The O₂ day glow is a result of the photolysis of ozone: about 90 % of ozone molecules produce oxygen at the $a^1\Delta_g$ state de-activated by emission or by collisions with the CO₂ molecules (below some level of the atmosphere).

Vertical profile of ozone number density is estimated from the limb profiles of the O₂ day glow with vertical resolution up to 1–2 km, taking into account the lost in collisions with the CO₂. The vertical profiles of the CO₂ number density are taken from the simultaneous PFS observations.

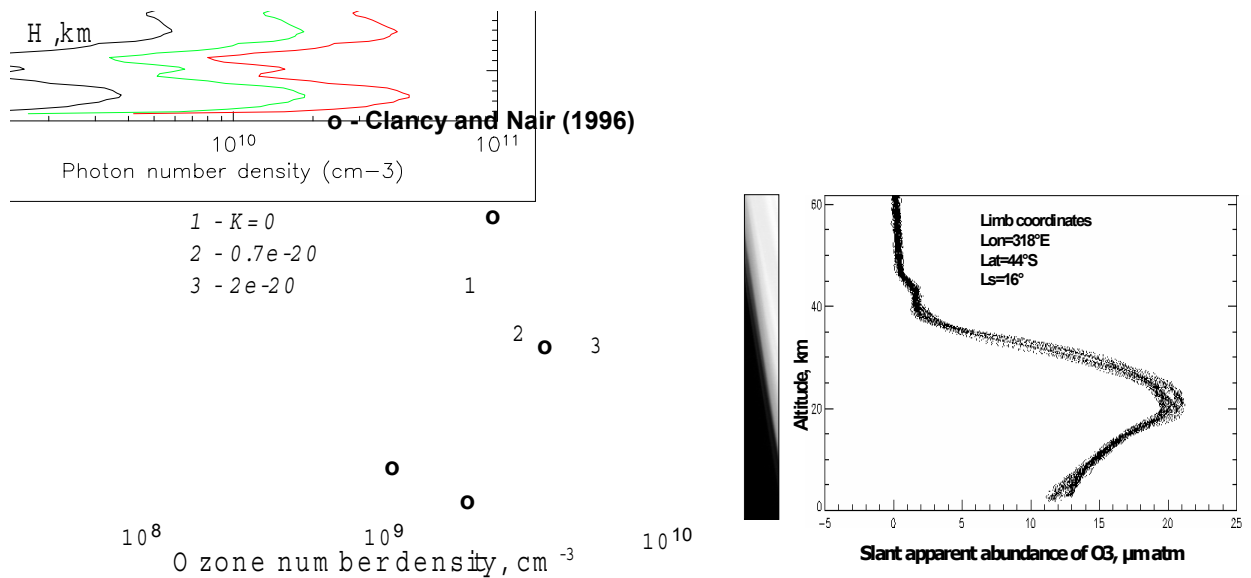


Fig. 4. The vertical profile of ozone above Argire and the slant apparent abundance of ozone: $\varphi = -44^\circ \text{N}$, $\lambda = 318^\circ \text{E}$, $L_s = 16^\circ$, $L_t = 10.8\text{h}$. This morning profile contain also a pick at 40–50 km — rest of night time ozone layer

3.5.1.5. Seasonal variation of the thermal structure of the Martian atmosphere

Planetary Fourier spectrometer being on the near polar allows the retrieval of the thermal field vs. latitude – altitude at each single orbit. PFS spectra allow self consistent temperature profile and aerosol opacity retrieval from a single spectrum or from an average over several spectra at the same orbit (to increase S/N).

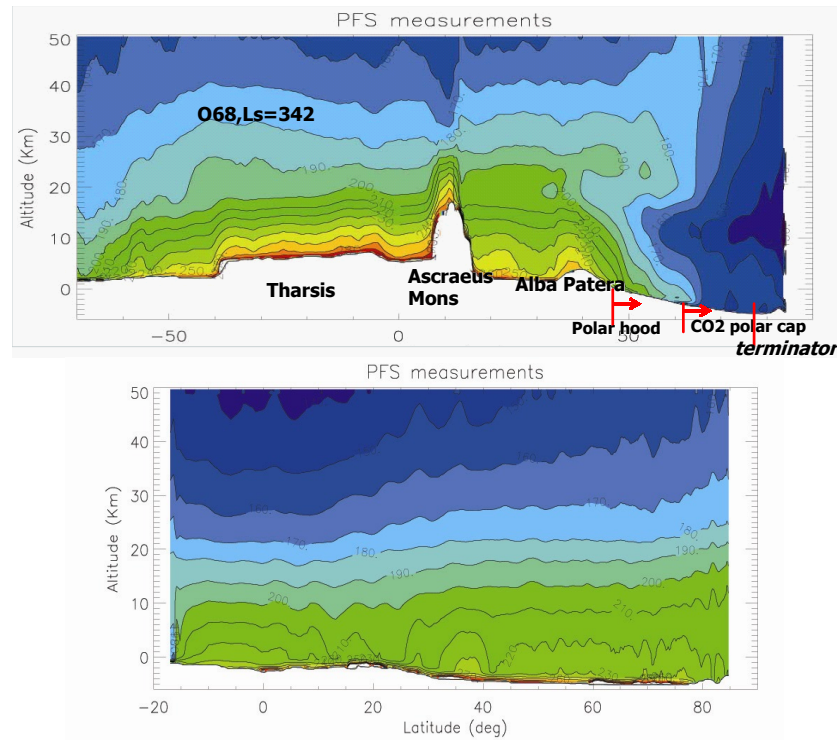


Fig. 5. Examples of the PFS temperature fields:
top — $L_s = 342^\circ$ (later Northern winter), bottom — $L_s = 97^\circ$ (summer)

Some important new finding

1. It was shown that the shape of the temperature profiles depends on the mode of global circulation. Elevated temperature inversion (at 10–20 km altitude) is found in the polar hood in descending branch of Hadley cell. This inversion in polar hood disappeared near equinox, when circulation changes.

2. Spectral resolution of PFS (1.8 cm^{-1}) with apodisation allow retrieval of the temperature profiles in the case of complex shape of temperature profile, when the temperature profiles have inversions. The temperature profiles for night (winter) in the polar regions, night observations in lowlands (like Hellas) and high lands (volcanoes) are retrieved.

3. The near isothermal shape of summer North polar temperature profile was found at low altitudes the surface and water ice clouds in the near surface layer. Above 20 km altitude the temperature increases with increasing latitude.

3.5.1.6. Dust and water ice clouds. PFS Mars Express

1. It was found that relief is important for aerosol observation in the atmosphere. It was found that at late southern summer along the orbit passing through lowlands only dust was observed, vertically distributed with the scale height of 11 km (on the average along the orbit from 70° S to 40° N). Along the orbit passing through volcanoes both water ice clouds and dust were observed, with water ice clouds dominate above volcanoes.

2. With PFS we observed several types of the H_2O clouds.

Orographic water ice clouds above volcanoes were observed with opacity from maximal of 0.5 (875 cm^{-1}) at late summer up to several units near aphelion and H_2O mass loading up to 60 ppm. Effective particle size changes from 1–3 μm , its variation was observed along the flanks of volcanoes.

Equatorial cloud belt was observed around aphelion with typical opacity averaged over FOV PFS of 0.1–0.5, reaching 2–3 and mass loading of 40–60 ppm in aphelion. It appears earlier (at $L_s = 25$) along the orbits passed through highlands.

Polar hoods. Ice clouds in polar hoods were observed with opacity up to several units and typical mass loading of 20–40 ppm. Elevated temperature inversion below 1mb level is found in both in Northern and Southern polar hoods. It is connected to the heating in the descending branch of Hadley circulation in winter.

Ice clouds above melting Northern polar cap were observed (for the first time we identify them from the PFS data) in the near surface layer in the northern polar region ($> 85^\circ$) with opacity of 1–2 and mass loading of 40–50 ppm.

Morning hazes. It was observed in Valles Marineris by PFS with opacity of 0.4–0.5 and mass loading of 5–7 ppm, with effective particle size of 2–3 μm . Simultaneous images of this haze were obtained by OMEGA and HRSC.

Night fogs. It was observed in Hellas near aphelion in the near surface layer (below temperature inversion) with opacity up to 3–5.

3.5.1.7. Research of the current Martian climate with Mars general circulation model

Mars General Circulation model (MGCM) developed on the basis of the GFDL Mars GCM has been modified in order to fit its output to available spacecraft data. Spatial resolution has been enhanced to $2 \times 2.4^\circ$ and the parameterization of coagulation and optical properties of aerosols has been improved. Assuming a hyperfine, submicron aerosol fraction allowed to improve agreement with the observed temperature field and to provide condensation nuclei for cloud formation.

Modeling of the water cycle on Mars has the purpose to reach the agreement with Mars Express observations; however, at the moment the model yields 2–3 times as much water in the tropical atmosphere as observed by SPICAM instrument. Latitude distribution of the water vapor and its seasonal trend qualitatively fits observations, although the quantitative agreement requires an additional source of dust in the polar latitudes, associated with the retreating polar cap, in order to damp the strength of the Hadley cell circulation. Studying of the contribution of stationary and quasi-stationary planetary waves in the meridional water transfer indicates that the areas of the enhanced hydrogen contents in Terra Arabia and to Southwest of Olympus Mons may be result from the accumulation of atmospheric water deposited in these locations by a stationary planetary wave with zonal wavenumber 2.

3.5.1.8. The model of charging and coagulation processes in Titan tholin haze

A 1-D microphysical model of the aerosols in Titan atmosphere taking into account photochemical production, collisional and photoelectric charging, coagulation, sedimentation and eddy mixing on the tholin particles has been developed. The model output, including vertical and size distribution of tholin nanoparticles (monomers), fractal aggregates, and subaggregates composing the internal structure of those aggregates, has been employed to obtain optical properties of the simulated haze, suitable for comparison with observational data. It is shown that nearly uniform vertical distribution of particles, their sizes and internal structure constrained by data of different channels of DISR spectral radiometer onboard Huygens lander, could be reproduced under assumption that particles are formed during Brownian coagulation controlled by electrostatic repulsion. A remarkably constant mean monomer radius, which varies within 0.05–0.06 μm , may result from the damping of Brownian coagulation of smaller particles by Coulombian potential created by a single elementary charge.

3.5.1.9. Russian experiment HEND onboard NASA Mars Odyssey

Russian instrument High Energy Neutron Detector (HEND) operates presently onboard NASA Mars Odyssey provided the data for neutron radiation from the Martian surface. Mars Odyssey was launched from the Cape Canaveral in April 2001 and in October of the same year it was inserted on the orbit around Mars (Fig. 6). HEND performs continuous orbital measurements from that time together with another science instruments on Mars Odyssey. HEND was developed in the Institute for Space Research by the contract with Federal Space Agency.



Fig. 6. NASA spacecraft Mars Odyssey with Russian instrument HEND onboard

Galactic cosmic rays freely penetrate into the Martian subsurface due to thin atmosphere of the Mars and produce secondary nuclear emission of neutrons and gamma-rays. Measurements of this emission from the orbit allow to estimate the content of the main soil-forming elements in the Martian soil. Neutron radiation is particularly sensitive to the presence of hydrogen in the subsurface, because hydrogen perform significant effect on neutron moderation during their diffusion leakage on the surface.

The major hydrogen bearing substance in the Martian soil is water, and therefore measurements of neutron emission from the circular polar orbit of Mars Odyssey allow to map the content of water (or water ice) in the subsurface of the read planet (Fig. 7).

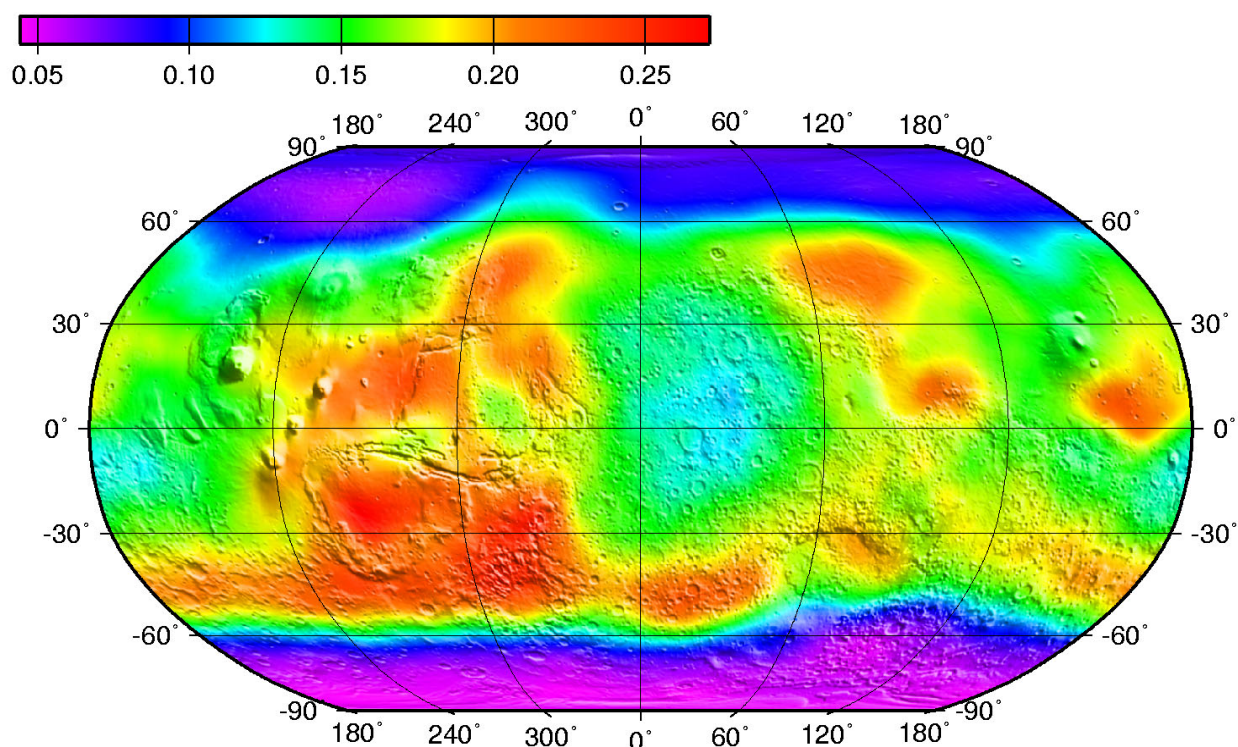


Fig. 7. The map of epithermal neutron emission from the surface of Mars from Russian instrument HEND onboard NASA Mars Odyssey. Different colors correspond to dynamic scale about 6 of different counting rate in the sensor MD with maximum at red and minimum at violet.

For high northern latitudes above 55° the data corresponds to the season of north summer

$L_s = 0-180^\circ$, for high southern latitudes above 55° the data corresponds to the season of north summer $L_s = 330-20^\circ$

If has been found from the data of Russian instrument HEND that content of water ice is larger than 30–50 wt% at latitudes higher than 60° , therefore the water ice is the major soil-forming substance there. Besides that, the high content of water up to 10 wt% has also been observed in the soil and the equatorial region of Arabia and in the region south-west from the Olympus Mountain (see Fig. 2). Results from HEND are important for understanding of the process of global evolution of Mars. These results will be taken into count for planning of future exploration mission to Mars as well.

Surface condensation of atmospheric carbon-dioxide in the winter changes the element composition of the layer of neutron emission. Therefore, measurement data from HEND allow to estimate the thickness of the layer of dry ice at different places on the surface of Mars. The seasonal profiles of surface condensation of CO₂ have been built according to HEND data both for north and south hemispheres (Figs. 3, 4).

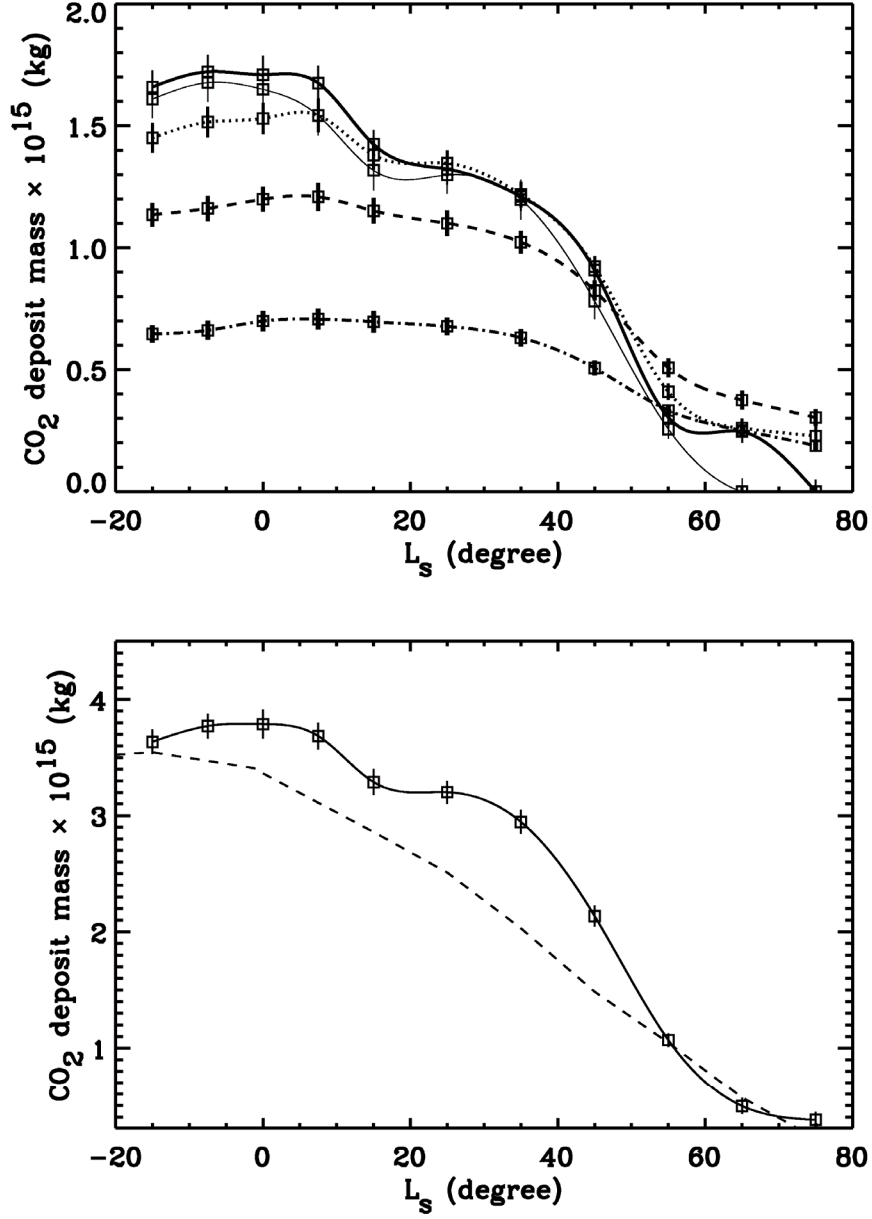


Fig. 8. Time-dependent variations of mass of surface condensation of CO₂ in the north hemisphere for different seasons of Martian year. Top plot: thin curve corresponds to condensed mass of CO₂ along the latitude belt of 60–70° N, bold curve corresponds to condensed mass of CO₂ along the latitude belt of 65–75° N, dotted curve corresponds to condensed mass of CO₂ along the latitude belt of 70–80° N, dashed curve corresponds to condensed mass of CO₂ along the latitude belt of 75–85° N, dashed-dotted curve corresponds to condensed mass of CO₂ along the latitude belt of 80–90° N. Bottom plot: solid line corresponds to seasonal variation of condensed mass at north according to neutron data and dashed line corresponds to prediction of GCM atmospheric model of Mars

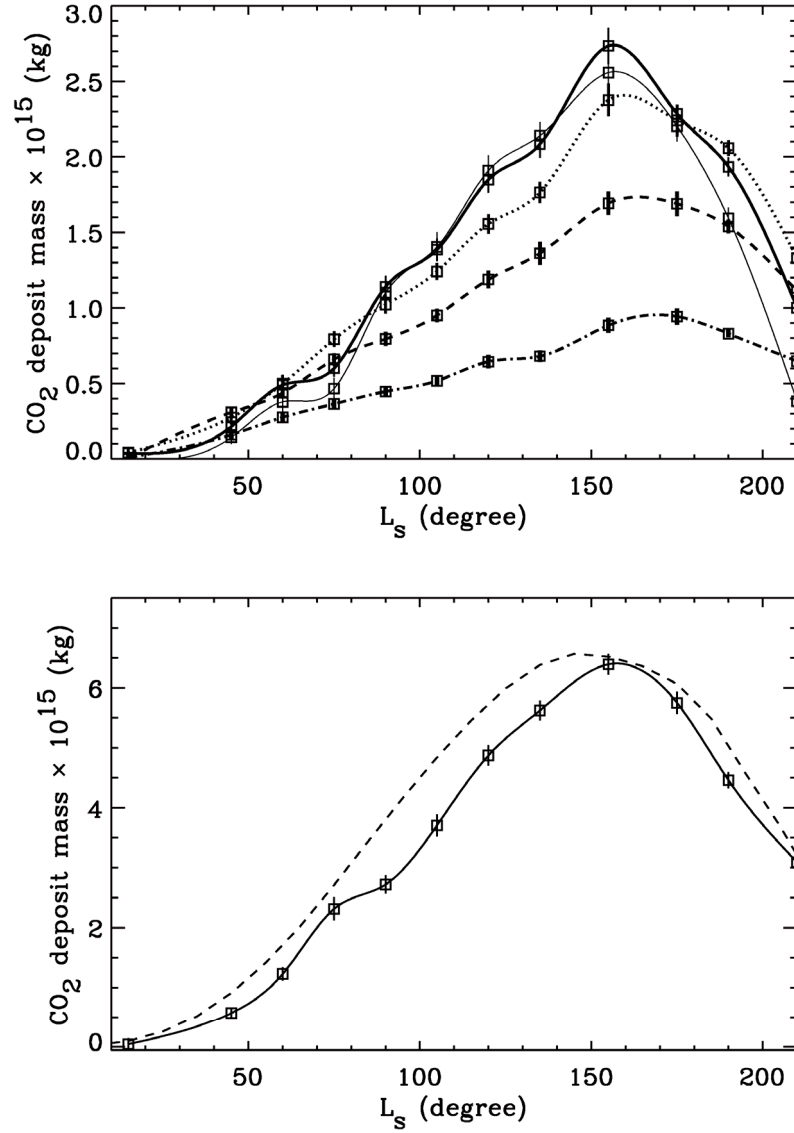


Fig. 9. Time-dependent variations of mass of surface condensation of CO₂ in the south hemisphere for different seasons of Martian year. Top plot: thin curve corresponds to condensed mass of CO₂ along the latitude belt of 60–70° S, bold curve corresponds to condensed mass of CO₂ along the latitude belt of 65–75° S, dotted curve corresponds to condensed mass of CO₂ along the latitude belt of 70–80° S, dashed curve corresponds to condensed mass of CO₂ along the latitude belt of 75–85° S, dashed-dotted curve corresponds to condensed mass of CO₂ along the latitude belt of 80–90° S. Bottom plot: solid line corresponds to seasonal variation of condensed mass at south according to neutron data and dashed line corresponds to prediction of GCM atmospheric model of Mars

Continuation of HEND experiment on Mars Odyssey in 2007–2009 would allow to get sufficient volume of data for testing the hypothesis of layering structure for water-bearing soil at wet regions of Mars around equator. These data could be useful to understand which forms of water (adsorbed water, bound water or free ice) dominate in the soil at low latitudes. Due to several years of orbital measurements from Mars Odyssey, one would be able to compare seasonal variations at north and south hemispheres and to conclude on the stability of the climate on Mars.